

RESEARCH ARTICLE

Application of Chaotic Signals for Improving the Performance of New Generation Ball Mills

MÜKREMİN AY¹, ONUR KALAYCI¹, MIROSLAV MAHDAL², MÜCAHİT TURHAN³,
SELÇUK COŞKUN⁴, FATİH ÇALIŞKAN⁵, İHSAN PEHLİVAN⁴,
AND SUNDARAPANDIAN VAIDYANATHAN^{6,7}

¹Mechatronics Engineering Department, Graduate Education Institute, Sakarya University of Applied Sciences, 54050 Sakarya, Turkey

²Department of Control Systems and Instrumentation, Faculty of Mechanical Engineering, VSB—Technical University of Ostrava, 70800 Ostrava, Czech Republic

³Metallurgical and Materials Engineering Department, Graduate Education Institute, Sakarya University of Applied Sciences, 54050 Sakarya, Turkey

⁴Department of Electrical and Electronics Engineering, Faculty of Technology, Sakarya University of Applied Sciences, 54050 Sakarya, Turkey

⁵Department of Metallurgical and Materials Engineering, Faculty of Technology, Sakarya University of Applied Sciences, 54050 Sakarya, Turkey

⁶Centre for Control Systems, Vel Tech University, Avadi, Chennai, Tamil Nadu 600062, India

⁷Centre of Excellence for Research, Value Innovation and Entrepreneurship (CERVIE), UCSI University, Kuala Lumpur 56000, Malaysia

Corresponding author: Sundarapandian Vaidyanathan (sundar@veltech.edu.in)

This work was supported by the Project Applied Research in the Area of Control, Measurement and Diagnostic Systems supported by the Ministry of Education, Youth and Sports, Czech Republic, under Grant SP2024/038.

ABSTRACT New Generation Ball Mills have started to be preferred in milling systems regarding energy efficiency in recent years. In this article, modernization studies have been carried out to ensure that the current new generation ball mill (NGBM) operates on a chaotic basis. In experimental studies, chaotic signals loaded on the PLC device moved the milling chamber chaotically on horizontal or circular axes. While the grinding chamber is moving at constant speeds in both the horizontal and circular axis in the current NGBM, the improved New Generation Ball Mill (INGBM) has gained the ability to move at constant or chaotic speeds in both horizontal and vertical axes. In this study, the milling chamber of INGBM has a constant frequency speed in the horizontal and circular axes in the first scenario, a chaotic system in the horizontal axis, and a constant frequency speed in the circular axis in the second scenario. In the third scenario, it was ensured that it was moved at constant frequency speed in the horizontal axis and with the chaotic system in the circular axis. Experimental studies were carried out on the milling of SiC powder, which was chosen as an example in all scenarios. Sieve Analysis method and Scanning Electron Microscope (SEM) analysis methods were used when examining the ground powders. For both methods, the best results were obtained in the horizontal axis constant frequency speed (35 Hz) and circular axis chaotic (23-27 Hz, Lorenz system) operating scenario. It is seen that INGBM is 42% better in the powder size criterion and 3.44% better in the energy efficiency criterion.

INDEX TERMS New generation ball mill, milling, chaos, chaotic signals, energy efficiency, homogeneity, SiC powder, sieve analysis, scanning electron microscopy (SEM), PLC device.

I. INTRODUCTION

Today, the rapid development of technology has brought developments in material production systems, as in every field. The main usage areas of advanced technology ceramic

The associate editor coordinating the review of this manuscript and approving it for publication was Adamu Murtala Zungeru¹.

materials are aerospace, communication, energy and automotive industries.

The need for advanced technology ceramic materials in terms of their mechanical, physical, and chemical properties is increasing. Due to their superior properties, the use of high-tech ceramics in the mentioned sectors is quite common. One of the important features of high-tech ceramics is that they are produced from powders with much smaller

grain sizes than traditional ceramics. High-tech ceramics contain ceramic powder in sizes below 1 micron. Due to this advanced ceramics feature, denser materials can be obtained [1].

Due to their resistance to high temperatures, chemicals, mechanical, and thermal stresses utilized in the fields, high-tech ceramics are used in the industry that relies on mechanical, nuclear, optical, thermal, and electrical-magnetic, among other sectors.

High-tech ceramics are classified in the industry according to hardness, thermal resistance, abrasion resistance, high elastic modulus, density and fracture toughness. High-tech ceramics, including TiN, ZrO₂, TiB₂, Si₃N₄, B₄C, TiC and SiC, are used in various technical areas such as armored vehicle and vest protective layers, wear-resistant machine components, orthopedic prostheses, auto parts, sports equipment, nozzles and cutting edges [2].

We can cite the progress in ceramic technology as an example of the development of silicon carbide in the last 20 years. Silicon carbide has high thermal shock resistance, conductivity, wear and creep resistance, hardness, low coefficient of thermal expansion and corrosion resistance. It is used in ceramic and metal matrix composites, ceramic coatings, ceramic rings and gaskets, and wear components in coated abrasives and memory discs [3], [4], [5]. In addition, in complex engineering applications, silicon carbide is preferred over tungsten carbide due to its resistance to wear. The use and competitiveness of silicon carbide in the industry are due to its lower production cost than other non-oxide ceramic materials [6], [7].

Today, there are different material production methods. One of these methods is material production by powder metallurgy. Production with powder metallurgy dates back to prehistoric times. Modern powder metallurgy technology began with production of tungsten carbide and bronze bearings. The acceleration of the studies has increased with the use of ferrous and non-ferrous materials. Providing special production opportunities and being economical and fast makes powder technology preferred. Another reason for the preference is that it produces organic and ceramic materials in structural applications. It is a production method used in different areas such as automotive, aircraft and space industry, marine, railway, electrical-electronics, construction machinery, sports equipment and health [8], [9], [10].

Powders smaller than 200 μm are used in powder metallurgy and are getting smaller yearly with the developing technology [11]. There is always a relationship between the powder production technique and the powder's microstructure, shape, chemical properties and size. Powders with certain properties are produced using different production methods. The relationship between the manufacturing techniques of certain powders and the powder metallurgy manufacturing technology is based on a strong link. Manufacturing techniques effectively determine the powder's physical properties to be produced. Therefore, the appropriate powder

selection should be made according to the part production plan [12]. The parameters controlled in powder metallurgy part production depend on the powder's shape, surface morphology and size [13].

Industrial milling is applied to grain sizes smaller than 25 mm. The tools used to pulverize the ore are called 'grinders' or 'mills'. Milling a material is defined as a critical engineering problem in industrial applications. This problem is considered an important research topic. Impact, crushing, shearing and friction force methods are used in ball mills, and the material is pulverized [14]. Industry milling processes can generally be done in dry and wet milling. The energy consumption is relatively higher by 30% in dry milling applications [15]. The high energy consumption in dry milling is because the fine ground grains clump faster and are disconnected from the milling medium, which slows down the milling. It is suggested that different chemical substances can be used to prevent agglomeration in dry milling methods [16]. Wet milling is preferred as the milling method in ore preparation plants. The type of mill commonly used in advanced milling processes is a conventional ball mill.

Due to the use of balls larger than 25 mm in ball mills, the energy to be transferred to the ground ore is not sufficient for milling in small sizes. Compression and shear forces are required to crush small particles. Milling up to 100 μm in ball mills can be considered within the economic milling limits. When it is below 100 μm , the energy consumption of ball mills increases considerably [17].

In milling processes, as the size decreases, the resistance of the grains to breakage increases, causing an excessive increase in the amount of energy consumed. In the studies on milling, the relationship between the energy consumed and size reduction has been examined. While a part of the energy consumed in traditional mills is used for size reduction, a significant part is lost as heat and sound. In addition, in advanced milling, the efficiency of conventional mills decreases, and milling becomes uneconomic [18].

The decrease in energy resources and the difficulty of accessing the resources have increased energy costs. Turning to new generation ball mills rather than traditional methods in milling systems is an important requirement. It is foreseen that the new generation of ball mills will contribute to the future of enterprises and the efficient use of energy resources.

Efforts are being made to reduce the costs since the energy required for milling is an important cost factor due to the negativity of traditional methods. In this context, cost reduction methods should be within the framework of following the new generation of technology. In traditional milling processes, when quality milling is desired by increasing the engine speed, this situation is, on the contrary, high energy loss and low efficiency [19].

Many new generation ball mills have been designed to reduce the milling cost and increase milling efficiency. These mills make economical milling possible even in milling processes below 10 microns. This is because the amount of

energy released per unit of time and volume in the stirred mill is very high, and the energy consumption is very low compared to conventional mills. High-pressure roller mills and vibratory mills stand out as alternatives to traditional mills.

In the new generation ball mill introduced by Gungordu, the milling chamber moves at constant speeds on the horizontal and circular axes. When the milling performances of the traditional ball mill, planetary mill, and new generation ball mill are compared, the weight of powder content below $32\ \mu\text{m}$ in the ball mill is 10%. In comparison, the weight of powder content below $32\ \mu\text{m}$ in the high-energy mill is over 50% [20]. The research showed that the performance of the new generation ball mill is better than that of traditional ball mills.

Chaos, also expressed as the order of disorder, is a branch of science that helps explain non-linear events and shows complex behaviors but has its internal order. Chaos and chaotic signals: Image processing features such as its sensitive dependence on initial conditions, containing an unlimited number of different periodic oscillations, irregularity in the time dimension, having a fragmented (fractal) dimension in the limit set, having a wide power spectrum similar to noise, and containing signals whose amplitude and frequency cannot be determined, but changing in a limited area. Its widespread use has played a major role in many areas, such as communication, optimization, fuzzy logic, mechatronics, physics, control, and encryption [21], [22], [23].

In recent years, chaotic signals have started to be used in areas such as milling and mixing because of their random behavior [21], [22], [23], [24], [25], [26], [27], [28], [29], [30], [31], [32], [33], [34], [35], [36], [37], [38], [39], [40], [41], [42]. Chaos theory can be expressed as a science field investigating the order of disorder. Chaotic systems display complex behaviors but have a secret order of their own. This indicates that the chaos event is not random [24]. The equations found in 1963 by meteorologist Lorenz from M.I.T. can be considered the first chaotic systems that show sensitive dependence on initial conditions. Chaos and Chaotic signals contain disorder in the time dimension, are sensitively dependent on initial conditions, contain an unlimited number of different non-periodic oscillations, and have a wide power spectrum like noise. However, the fact that the limit set is fragmented, and contains signals whose amplitude and frequency cannot be determined, but that change in a defined area are important features of chaos [25].

Chaotic systems can be classified as autonomous and non-autonomous systems. The state variable depends on time(t) in non-autonomous chaotic systems. In autonomous chaotic systems, the state variables are independent of time [26].

In the literature, non-autonomous chaotic systems and many autonomous chaotic systems have also been introduced. Autonomous chaotic systems include the Chua oscillator [27], Lorenz system [25], Mobayen systems [28], Chen

system [29], Sprott-A system [30] and Pehlivan-Wei system [24] can be given as examples.

In recent years, its use has been increasing in many fields, such as chaos theory, communication security [31], cryptology [32], industry [23], weather forecasts [33] and random number generators [34]. Chaos theory aims to explain the underlying order in seemingly random patterns, focusing on understanding systems that contain uncertainty and disorder.

Quality mixing (confusion) and diffusion (diffusion) are two basic requirements to ensure homogeneity in mixing processes. The complex dynamical properties of chaotic systems are important elements that will ensure dispersion and quality mixing. Various studies have been carried out to increase the efficiency of mixers used in the industry by taking advantage of these features of chaotic systems [35], [36], [37], [38], [39], [40], [41], [42]. In their study, Kalayci et al. controlled the speed of the mixer they designed to obtain humic acid from leonardite with both chaotic systems and traditional methods. They found that the mixing done with the chaotic system was compared to that done with traditional methods in terms of criteria such as homogeneity, time, product quality and energy saving. They observed that it was more efficient [35]. Kalayci et al. designed a new chaotic mixer based on a delta robot controlled by the Arduino Uno R3 board and MATLAB. They found that the homogeneity and orbital distribution ratio (SDO) parameters obtained for a solid-liquid mixture type were obtained using seven different chaotic systems at the selected mixing time. They conducted comparative and experimental studies [36]. In his study, Kurt examined whether chaotic mixers that work less and consume less power can obtain a mixture with a higher homogeneity rate [37]. Chau et al. compared the results of chaotic mixing with constant speed mixing using a feedback DC motor in which the rotation speed is adjusted chaotically [38]. In their study, Ye and Chau compared the results of chaotic mixing with the results of mixing at a constant speed using a DC motor in which the rotation speed is adjusted chaotically by the destabilization method [39]. In their study, Murtadha et al. mixed a water-salt mixture in a chaotically controlled liquid mixer for 30 s. They mixed the mixture and evaluated the results by making concentration measurements. [40]. In their study, Zhang and Chen designed a mixer in which the blades used in the mixer were kept fixed, and instead, the chamber containing the mixture was rotated with a DC motor. The mixer motor's speed was adjusted chaotically using the Chua circuit, and a water-sugar mixture was used in the experiments [41]. In their study, Kavur et al. mixed graphene nanoplatelets by designing a chaotic system-based Delta Robot [42].

In the studies on mixers in the literature, similar improvements can be achieved regarding criteria such as powder size and energy efficiency in milling processes since better homogeneity and time and energy savings have been successfully achieved using chaotic signals. An exemplary design and experimental studies of the chaotic movement of the milling



FIGURE 1. New generation ball mill.

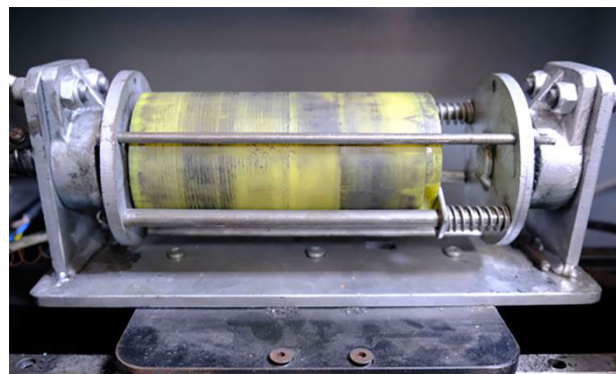


FIGURE 2. Powder milling chamber.

chamber on the horizontal and circular axis, with the help of chaotic signals received from the PLC device, are presented.

The rest of this research paper is as follows. In Parts II A, B, and C, the pre-improvement structure of the current new generation ball mill and the modernization stages of the ball mill by creating chaotic data are explained. Part II D covers the grinding ring's characteristics and the ground powder's properties. Part II E compares traditional ball mills and New Generation Ball Mills. Part III A and Part III B are experimental studies on bringing chaotic motion to the INGBM in the horizontal and circular axis. The article ends with a summary of the results and discussion sections.

II. MATERIALS AND METHODS

A. NEW GENERATION BALL MILL EXISTING BEFORE IMPROVEMENT (NGBM)

The new generation ball mill, which was improved in this article, was introduced by Gungordu [20] in 2018 (Figure 1). The milling chamber moves in the horizontal and circular axes at constant frequency speeds. The milling process is carried out by moving the milling chamber at high speeds in the horizontal and circular axis, with the help of many steel balls in the chamber. The balls used in the powder milling process are made of stainless steel, and their diameter is 8 mm.

Negative conditions such as powder heaps and cold fusion caused by the powder material placed in the milling chamber when the chamber moves only on the horizontal axis are eliminated by giving circular motion to the chamber.

The milling chamber (Figure 2), in which the powder milling process is carried out, containing the powder and steel balls, is made of hard plastic, and there is a suitable mechanism for the bed on which the powder chamber is located to provide horizontal movement easily. The grinding chamber has a length of 150 mm, an outer diameter of 80 mm and a wall thickness of 5 mm. The crank-connecting rod mechanism provides the movement required for this process.

To ensure the horizontal and circular movement of the existing milling chamber, two asynchronous motors and

drivers can operate at speeds between 0-3000 rpm in the machine.

Asynchronous motors are operated by a control unit containing a PLC device. A vibrating sieve was used to separate the powders ground in the system. Due to the movement of the milling chamber in the horizontal and circular axis in the current new generation ball mill, the powders exposed to the crushing force are transformed into smaller sizes in a much shorter time than conventional ball mills, thanks to the balls moving more randomly.

At INGM, PLC and inverters were inside the grinding machine. The vibration during the grinding negatively affected the operation of the PLC and inverters. In the developed system, the control unit, which consisted of PLC and inverters, was removed from the grinding machine, and an independent control unit was created.

B. IMPROVED NEW GENERATION BALL MILL (INGBM)

Converting chaotic time signals to frequency data is aimed at improving the powder size and energy efficiency criteria compared to conventional ball mills by randomly changing the speed of the milling motors. To grind Silicon Carbide (SiC) powder, which was chosen as an example in the study, several innovations were made in the existing NGBM control unit, and a PLC-controlled prototype new generation ball mill was designed and modernized, all functions of which can be controlled by the HMI Operator panel in Figure 3.

First, the machine's PLC device was replaced with a newer model. Later, this unit was located outside the milling part of the machine so that the control unit was much less affected by machine vibrations. At the same time, the frequency inverter in the current system drives two asynchronous motors on the horizontal and vertical axes alone. The new system used two inverters to drive the motors separately, with constant frequency or chaotic speed options.

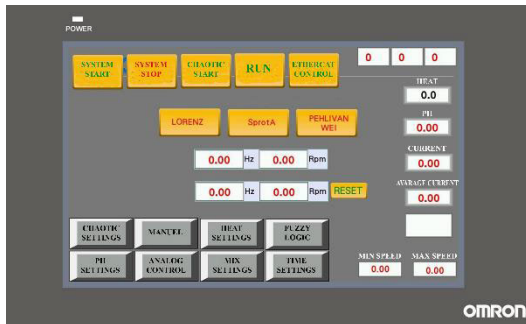
The PLC used in the system before modernization is the DELTA brand DVP 14 SS2 model. This model is the most basic model of the PLC brand and is unsuitable for use in the new system.



a) Milling Machine



(b) Control Unit



(c) HMI Operator Panel

FIGURE 3. Improved new generation ball mill.

Omron brand NX1P2-9024DT1 model PLC was used as the control device in the modernized system. The PLC has an SD CARD slot compatible with the ETHERCAT communication protocol. After the chaotic data obtained from the CESSP program are saved in the SD CARD in txt format, they are converted into chaotic frequency data with the algorithm written in the PLC. The obtained frequency data were transferred to Omron brand ethercat controlled 3G3AX-MX2-ECT model inverters used in horizontal and circular motors via ethercat communication protocol, enabling the motors to be operated with chaotic frequencies.

As can be seen from the block diagram of the INGBM system (Figure 4), the time series signals of the chaotic systems, which are first solved in the MATLAB program, are uploaded to the SD card in the PLC device. Thanks to the PLC and operator panel software developed in the study, for each of the motors on the horizontal and circular axis, whether they will be operated at constant speed or chaotic speed; if it is to be operated chaotic, which chaotic system and in which frequency range it will work; If constant speed is selected, it can be determined at what frequency it will operate and what the sampling step interval will be in each selected chaotic system.

After selecting the sample operation scenario settings on the HMI operator panel, asynchronous motors on the horizontal and circular axis can be operated at a constant frequency speed frequency or chaotic frequency speeds via frequency inverters with the signals received from the PLC device.

Inside the INGBM control unit, there are HMI operator panel, Omron 0.75 kW frequency inverters (as shown in Figure 5), Omron NX1P2-9024DT1 PLC device (as shown in Figure 6), two asynchronous motors that can operate at speeds between 0-3000 rpm, and a power source to provide electrical energy to the system.

There is also an HMI operator panel where the motor speeds in the horizontal and circular axes can be adjusted separately as fixed frequency speed or chaotic.

C. MODERNIZING THE BALL MILL BY CREATING CHAOTIC DATA

NGBM has been modernized by enabling the engines to be operated at variable speeds with the help of chaotic signals. For this purpose, a chaotic equation solution and simulation program (CESSP), which works according to a numerical solution algorithm, was developed using the LabView program to obtain velocity data from chaotic orbits.

Various methods have been developed in the literature to solve differential equations numerically. Euler, Heun and Runge-Kutta methods can be given as examples of these methods. Euler’s algorithm is the simplest method developed for numerical solutions of differential equations. However, Euler’s algorithm generally cannot produce very precise solutions. Also, since chaotic systems are sensitively dependent on initial conditions, a very small change in initial conditions significantly changes the system’s dynamic behavior. For this reason, the Runge-Kutta (RK4) algorithm [43], which has high accuracy and fast convergence features and produces more accurate results for the numerical solution algorithm, is used in the CESSP program. The equations for the implementation of the RK4 algorithm are shown in Equation (1).

$$\begin{aligned}
 y_{k+1} &= y_k + \frac{h}{6} (\kappa_1 + 2\kappa_2 + 2\kappa_3 + \kappa_4) \\
 \kappa_1 &= F(x_k + y_k) \\
 \kappa_2 &= F\left(x_k + \frac{h}{2}, y_k + \frac{h}{2}\kappa_1\right)
 \end{aligned}$$

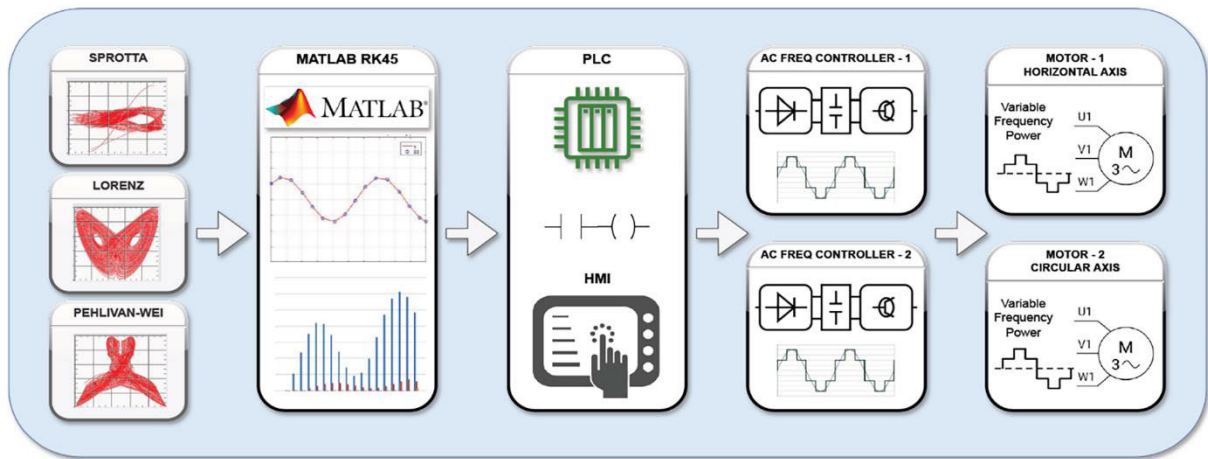


FIGURE 4. Block diagram of the INGBM system.



FIGURE 5. Omron 0.75 kW frequency inverters in the control unit.



FIGURE 6. Omron NX1P2-9024DT1 PLC.

$$\begin{aligned} \kappa_3 &= F\left(x_k + \frac{h}{2}, y_k + \frac{h}{2}k_2\right) \\ \kappa_4 &= F(x_k + h, y_k + hk_3) \end{aligned} \quad (1)$$

The discretized mathematical model of the chaotic systems selected with the RK4 algorithm is given in Equation (2) [43].

$$\begin{aligned} x(k+1) &= x(k) + \frac{1}{6}h[\kappa_1(k) + 2\kappa_2(k) + 2\kappa_3(k) + \kappa_4(k)] \\ y(k+1) &= y(k) + \frac{1}{6}h[\lambda_1(k) + 2\lambda_2(k) + 2\lambda_3(k) + \lambda_4(k)] \\ z(k+1) &= y(k) + \frac{1}{6}h[\xi_1(k) + 2\xi_2(k) + 2\xi_3(k) + \xi_4(k)] \end{aligned} \quad (2)$$

The parameters $\kappa_1, \kappa_2, \kappa_3, \kappa_4$ in (2) are the coefficients of the Runge-Kutta (RK4) algorithm belonging to the first equation of the selected chaotic system, $\lambda_1, \lambda_2, \lambda_3, \lambda_4$ parameters are the coefficients of the RK4 algorithm belonging to the second equation of the chaotic system and the parameters $\xi_1, \xi_2, \xi_3, \xi_4$ are the coefficients of the RK4 algorithm belonging to the third equation of the chaotic system.

By placing these coefficients $\kappa_i, \lambda_i, \xi_i (i = 1, 2, 3, 4)$ in the Runge-Kutta (RK4) algorithm, the extended mathematical model of the chaotic system in Equation (3) is obtained [43].

$$\begin{aligned} \kappa_1 &= f(x(k), y(k), z(k)) \\ \lambda_1 &= g(x(k), y(k), z(k)) \\ \xi_1 &= \delta(x(k), y(k), z(k)) \\ \kappa_2 &= f\left(x(k) + \frac{1}{2}h\kappa_1, y(k) + \frac{1}{2}h\lambda_1, z(k) + \frac{1}{2}h\xi_1\right) \\ \lambda_2 &= g\left(x(k) + \frac{1}{2}h\kappa_1, y(k) + \frac{1}{2}h\lambda_1, z(k) + \frac{1}{2}h\xi_1\right) \\ \xi_2 &= \delta\left(x(k) + \frac{1}{2}h\kappa_1, y(k) + \frac{1}{2}h\lambda_1, z(k) + \frac{1}{2}h\xi_1\right) \\ \kappa_3 &= f\left(x(k) + \frac{1}{2}h\kappa_2, y(k) + \frac{1}{2}h\lambda_2, z(k) + \frac{1}{2}h\xi_2\right) \\ \lambda_3 &= g\left(x(k) + \frac{1}{2}h\kappa_2, y(k) + \frac{1}{2}h\lambda_2, z(k) + \frac{1}{2}h\xi_2\right) \\ \xi_3 &= \delta\left(x(k) + \frac{1}{2}h\kappa_2, y(k) + \frac{1}{2}h\lambda_2, z(k) + \frac{1}{2}h\xi_2\right) \\ \kappa_4 &= f(x(k) + h\kappa_3, y(k) + h\lambda_3, z(k) + h\xi_3) \\ \lambda_4 &= g(x(k) + h\kappa_3, y(k) + h\lambda_3, z(k) + h\xi_3) \\ \xi_4 &= \delta(x(k) + h\kappa_3, y(k) + h\lambda_3, z(k) + h\xi_3) \end{aligned} \quad (3)$$

Differential equations of the chaotic systems [23], [24], [25], [26], [27], [28], [29], [30], [31], [32], [33], [34], [35], [36] with different dynamic properties, selected from the literature for chaotic mixing experiments with the CESSP program, are solved according to the RK4 algorithm with the

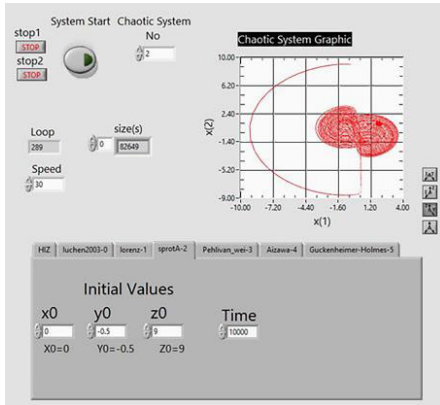


FIGURE 7. CEESP program.

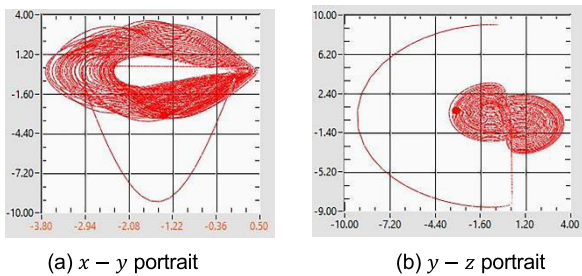


FIGURE 8. Phase portraits of the sprott A chaotic system obtained in the CEESP Program.

help of MATLAB script codes added to the program using x_0, y_0 and z_0 initial values, and x, y, z chaotic time series results of each chaotic system and $x - y, x - z, y - z, x - y - z$ phase portraits can be obtained as shown in Figure 7.

To determine the most suitable chaotic system for experimental studies, a selection was made between the Lorenz system, Sprott A system and Pehlivan-Wei chaotic system according to their average milling speed.

First, we consider the Sprott A chaotic system given by the Equation (4) dynamics [30].

$$\begin{aligned} \dot{x} &= y \\ \dot{y} &= -x + yz \\ \dot{z} &= 1 - y^2 \end{aligned} \quad (4)$$

We take the initial conditions as $x(0) = 0, y(0) = 0.5$ and $z(0) = 9$.

The $x - y$ and $y - z$ phase portraits of the Sprott A chaotic system, obtained by solving the differential equations given in Equation (4) using the RK4 numerical algorithm in the CEESP program, are as shown in Figure 8. The time series of the Sprott A chaotic system are given in Figure 9.

Next, we consider the Lorenz chaotic system, which the Equation defines (5) dynamics [25].

$$\begin{aligned} \dot{x} &= 10(y - x) \\ \dot{y} &= -xz + 28x - y \end{aligned}$$

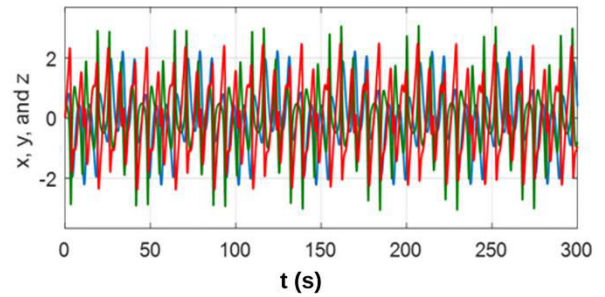


FIGURE 9. Chaotic variation of the x, y, z variables of the sprott A chaotic system.

$$\dot{z} = xy - \left(\frac{8}{3}\right)z \quad (5)$$

We take the initial conditions as $x(0) = 0, y(0) = -0.1$ and $z(0) = 9$.

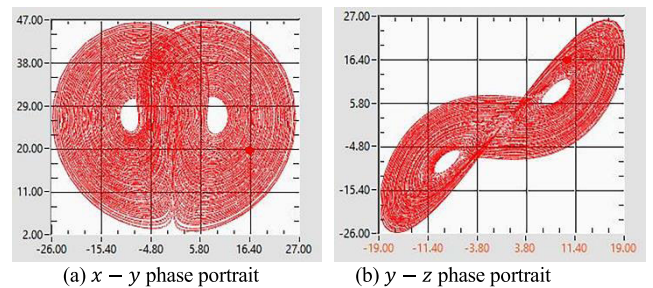


FIGURE 10. Phase portraits of the Lorenz chaotic system obtained in the CEESP program.

The $x - y$ and $y - z$ phase portraits of the Lorenz chaotic system, obtained by solving the differential equations given in Equation (5) using the RK4 numerical algorithm in the CEESP program, are as shown in Figure 10. The time series of the Lorenz chaotic system are given in Figure 11.

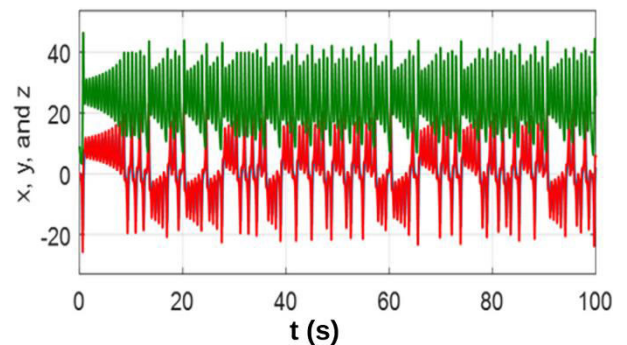


FIGURE 11. Chaotic variation of the x, y, z variables of the Lorenz chaotic system.

Next, we consider the Pehlivan-Wei chaotic system, which the Equation defines (6) dynamics [24].

$$\begin{aligned} \dot{x} &= y - yz \\ \dot{y} &= y + yz - 2x \\ \dot{z} &= 2 - xy - y^2 \end{aligned} \quad (6)$$

We take the initial conditions as $x(0) = -4, y(0) = 1$ and $z(0) = -4$.

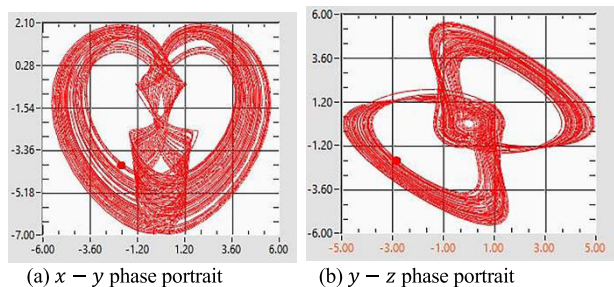


FIGURE 12. Phase portraits of the Pehlivan-Wei chaotic system obtained in the CESSP program.

The $x - y$ and $y - z$ phase portraits of the Pehlivan-Wei chaotic system, obtained by solving the differential equations given in Equation (6) using the RK4 numerical algorithm in the CESSP program, are as shown in Figure 12. The time series of the Pehlivan-Wei chaotic system are given in Figure 13.

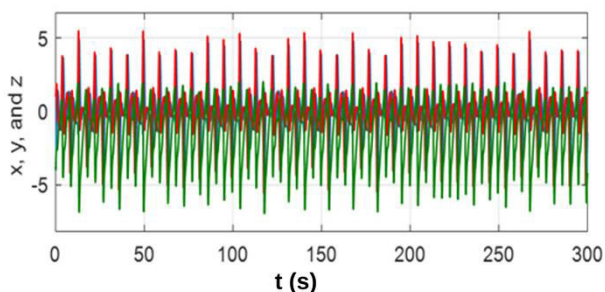


FIGURE 13. Chaotic variation of the x, y, z variables of the Pehlivan-Wei chaotic system.

1) INTEGRATION OF CHAOTIC SIGNALS INTO INGBM

A PLC software that converts the chaotic time series results obtained from the CESSP program into frequency data and, according to this data, enables the ball mill motors controlled by the frequency inverter in INGBM to rotate at varying speeds according to the chaotic systems selected via the operator panel, was developed using the Sysmac Studio PLC software platform. PLC software provides speed limits for motors, operating currents, instantaneous speed information, current values, operating time settings, etc. It allows us to manage data.

A program was written in the “Lorenz, SprottA, Pehlivan-Wei” subprograms shown in Figure 14, in txt file format, which was copied to the SD card placed in the PLC, and which allows the time series results obtained from the CESSP program to be read at the time intervals set on the operator panel.

The $x, y,$ and z time series results obtained through the program are saved as output in Microsoft Excel format to be converted into chaotic velocity data. The X time series results

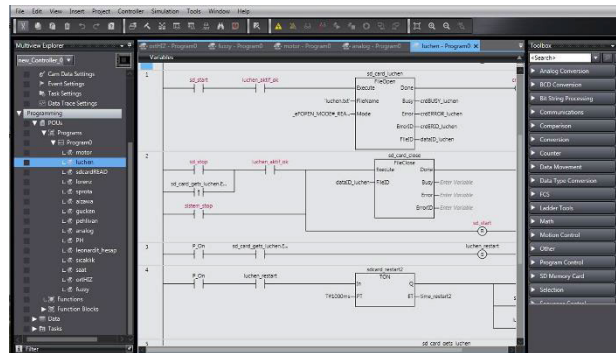


FIGURE 14. “Lorenz” subroutine.

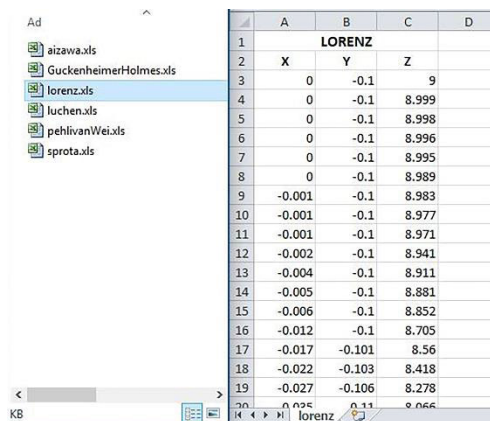


FIGURE 15. x, y, z coordinates of the Lorenz chaotic system.

shown in Figure 15 are saved in “.txt” format and copied to the SD card in the PLC [23], [24], [25], [26], [27], [28], [29], [30], [31], [32], [33], [34], [35], [36].

The chaotic system where the ball mill wants to be operated is selected among three different chaotic systems with the buttons on the “Chaotic Settings” screen shown in Figure 16. The minimum-maximum speed limits of the selected chaotic systems and the change times of the speed data coming from the coordinates of the chaotic system during grinding are also set on this screen.

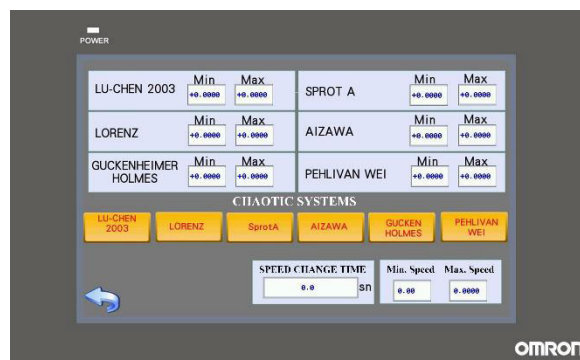


FIGURE 16. HMI “Chaotic Settings” screen.

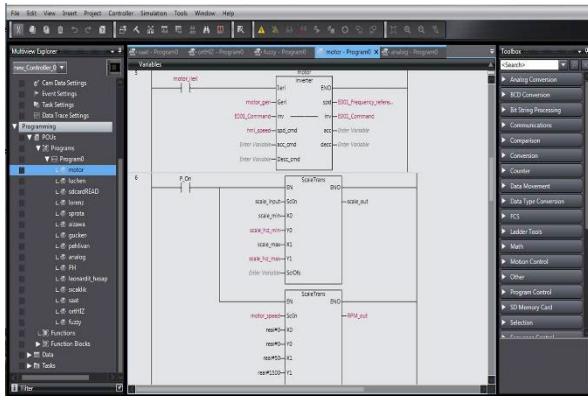


FIGURE 17. “Engine 1” subroutine.

The “Engine 1” subroutine in Figure 17 includes sending start, stop and speed data to the frequency inverter for the circular axis, receiving average current and error data, and scaling the time series results obtained from the CEES program between the minimum and maximum values entered from the operator panel. It was written to perform data conversion operations.

In addition, it is possible to control the ball mill motors, start the grinding process with the specified chaotic system, control the frequency inverter with ethercat, reset the speed information and move to other screens with the buttons on the screen in Figure 18. In addition, the instantaneous speed of the motors, the average speed during the grinding, the instantaneous current drawn, the average current drawn during the grinding, the minimum and maximum speed limits of the selected chaotic system and time information can be monitored in hours, minutes and seconds.

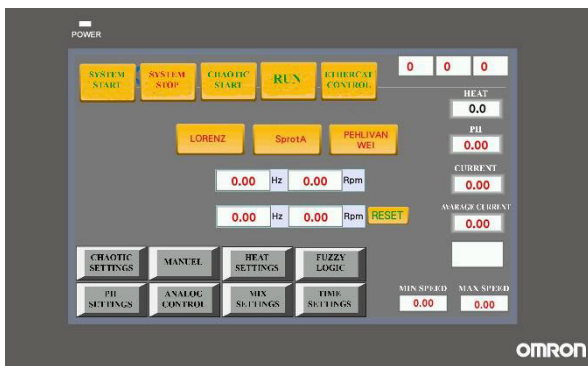


FIGURE 18. HMI “MONITOR” screen.

D. THE MILLING CHAMBER AS THE BASIS OF THE EXPERIMENT

The milling chamber, which is the basis of the system, moves horizontally and circularly. Thanks to the movement of the ball mill on the horizontal axis, the milling process is carried out by moving the tube back and forth at high speeds on the horizontal axis with the help of the balls used. The

crank-connecting rod mechanism provides the movement required for this process.

The powder materials in the milling tube move on the horizontal axis. Negative conditions such as powder piles and cold boiling that may occur during movement will be eliminated with the help of balls in the tube.

As a result of the movement of the chamber on the horizontal and circular axis, the powders exposed to the crushing force are transformed into small sizes in a much shorter time than the traditional methods.

Silicon carbide powder with suitable hardness was selected for milling. The size of silicon carbide powder before milling is 120–140 μm. The properties of silicon carbide powder are listed in Table 1.

TABLE 1. Properties of the silicon carbide powder.

Qualification	Value
Composition	SiC
Molecular weight (g/mol)	40.097
Color	green close to yellow
Intensity (g/cm3)	3.211
Melting Temperature	~2545 °C (at 1 atm)
Vickers Hardness (GPa)	24.5-28.2
Modulus of Elasticity	441-475
Shear Module (GPa)	192
Volume (Bulk) Module	96.6
Poisson Ratio	0.142
breaking strength (MPa)	350-600
Chemical Resistance	Room temperature

E. COMPARISON OF NGBM WITH CONVENTIONAL BALL MILL AND PLANETARY BALL MILL

With NGBM, the conventional ball mill and planetary mill were operated separately at 35 Hz (2100 rpm) and 90 minutes, and the results were compared in the graph in Figure 19. The graph shows that the amount of powder below 32 μm was over 50% in NGBM. Powder below 32 μm in the planetary mill closest to it. It was around 35%. In the ball mill, the powder content is below 32 μm. It could not even reach 10%. The results show that the NGBM is more efficient than the ball mills in its class with conventional mills [20].

III. EXPERIMENTAL STUDIES AND RESULTS

A. INGBM’S STUDY AND SIEVE ANALYSIS METHOD

INGBM has two asynchronous motors that enable operation in horizontal and circular axis. While the asynchronous motor, which provides movement on the horizontal axis, operates at a constant speed with a frequency of 35 Hz, in the chaotic system it operates in the frequency range of 33 Hz to 37 Hz. While the asynchronous motor, which provides movement in the circular axis, operates at a constant speed

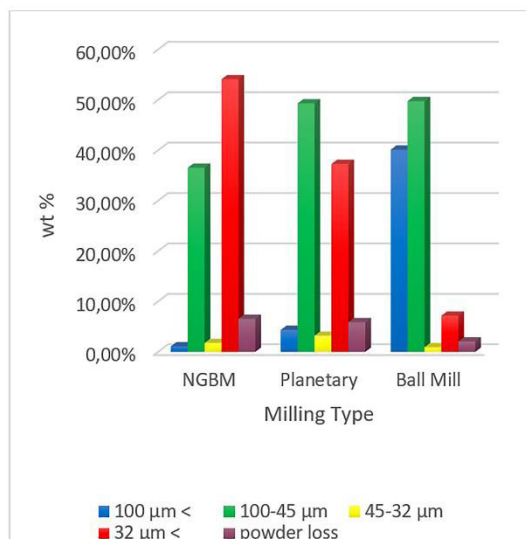


FIGURE 19. Comparison chart according to ground powders (90 min).

with a frequency of 25 Hz, in the chaotic system it operates in the frequency range of 23 Hz - 27 Hz.

In the sieve analysis method, three sieves of 100 μm, 45 μm and 32 μm sizes were used to determine the grinded powder sizes. The sieving process was shortened by using a sieve-shaking machine. The powders obtained during the sieving process were separated according to their sizes, calculated as % by weight, and tables were prepared.

1) INGBM'S OPERATION RESULTS WITH FIXED FREQUENCY ON THE HORIZONTAL AXIS AND CIRCULAR AXIS

A PLC software, which converts the chaotic time series results obtained from the CESSP program to frequency data and enables the horizontal and circular motors controlled by frequency inverters in INGBM to rotate at varying speeds according to the chaotic systems selected on the operator panel, has been developed using the Sysmac Studio PLC software platform.

With the software written using the Sysmac Studio PLC software program, the X coordinate of the chaotic system selected on the operator panel is sent to the frequency inverters at adjustable time intervals after scaling at the set minimum and maximum speed ranges, allowing the horizontal and circular motion motors to rotate at variable speeds. The aforementioned chaotic systems are preferred to be operated in the ball mill with a frequency range of minimum 23 Hz and maximum 27 Hz on the circular axis, and a minimum frequency of 33 Hz and a maximum of 37 Hz on the horizontal axis for 15 minutes. Initially, while the horizontal axis ran at a constant speed of 35 Hz, the circular axis's chaotic systems were tested. Afterward, while the circular axis operated at a speed of 25 Hz, the horizontal axis's chaotic systems were tested. Obtained results are shown in the tables.

The new generation ball mill, the efficiency of which is shown in the graph in Figure 19, was modernized to operate

with chaotic signals, and the SiC powder was ground by operating at a constant speed of 35 Hz on the horizontal axis and at a constant speed of 25 Hz on the circular axis for 15 minutes. After milling, sieve analysis was performed for 60 minutes, powder size and energy efficiency were measured, and the results are shown in Table 2.

TABLE 2. Milling results with horizontal axis = 35 Hz (Constant frequency speed), Circular axis = 25 Hz (Constant frequency speed).

Particle Size Range (μm)	Distribution of the Powder Amount (%) wt)	Distribution of the Powder Amount (g)
100 μm +	81,75 %	51,69
100 – 45 μm	15,16 %	9,59
45 – 32 μm	1,23 %	0,77
- 32 μm	1,86 %	1,18

The amount of powder, 65 grams before the experiment with a constant speed of 35 Hz on the horizontal axis and 25 Hz on the circular axis for 15 minutes, decreased to 63.23 grams at the end of the grinding. Its weight was measured as 240 65 grams at the end of grinding. The ground powders' appearance is classified according to size, as shown in Figure 20. During the 15-minute experiment, the system's energy consumption was measured as 0.581 kWh.

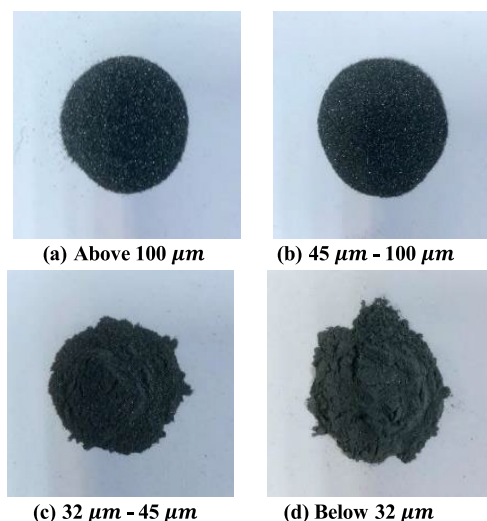


FIGURE 20. Horizontal axis 35 Hz (Constant frequency speed), Circular axis 25 Hz (Constant frequency speed), Image of ground powders.

2) INGBM'S OPERATION RESULTS WITH CHAOTIC SYSTEM ON THE HORIZONTAL AXIS AND FIXED FREQUENCY ON THE CIRCULAR AXIS

By integrating the chaotic system into INGBM, the circular axis was kept at a constant speed of 25 Hz, while the grinding process was carried out for 15 minutes using three different

TABLE 3. Horizontal axis Lorenz system (In the range of 33-37 Hz, average 35.34 Hz), circular axis = 25 Hz (Constant frequency speed).

Particle Size Range (μm)	Distribution of the Powder Amount (% wt)	Distribution of the Powder Amount (g)
100 μm +	82.73 %	52.79
100 – 45 μm	13.87 %	8.85
45 – 32 μm	0.73 %	0.47
- 32 μm	2.67 %	1.70

chaotic systems (Lorenz, Sprott A and Pehlivan-Wei systems) at chaotic variable speeds between 33 Hz and 37 Hz on the horizontal axis. Afterward, a 60-minute sieve analysis was performed. The powder size and energy efficiency were measured, and the results are shown in Table 3 for the Lorenz System, Table 4 for the Sprott-A system and Table 5 for the Pehlivan-Wei system.

TABLE 4. Horizontal axis Sprott-A system (In the range of 33-37 Hz, average 35.60 Hz) circular axis = 25 Hz (Constant frequency speed).

Particle Size Range (μm)	Distribution of the Powder Amount (% wt)	Distribution of the Powder Amount (g)
100 μm +	82.32 %	54.41
100 – 45 μm	14.10 %	8.97
45 – 32 μm	0.86 %	0.55
- 32 μm	2.72 %	1.73

TABLE 5. Horizontal axis Pehlivan-Wei system (In the range of 33-37 Hz, average 34.92 Hz) circular axis = 25 Hz (Constant frequency speed).

Particle Size Range (μm)	Distribution of the Powder Amount (% wt)	Distribution of the Powder Amount (g)
100 μm +	83.81 %	54.00
100 – 45 μm	13.00 %	8.37
45 – 32 μm	0.46 %	0.30
- 32 μm	2.73 %	1.76

While the Lorenz chaotic system was operated for 15 minutes at a constant speed of 25 Hz on the circular axis and at a frequency varying between 33 Hz and 37 Hz on the horizontal axis, the powder amount, which was 65 grams before the test, decreased to 63.81 grams at the end of the grinding,

their total weight before the experiment was 240.52 grams. The weight of 115 balls, with a diameter of 8 mm, which is 8 mm in diameter, was measured as 240 48 grams at the end of grinding. During the 15-minute experiment, the system’s energy consumption was measured as 0.567 kWh. The milling results for the Lorenz system are presented in Table 3.

Sprott-A chaotic system with a constant speed of 25 Hz on the circular axis and a frequency varying between 33 Hz and 37 Hz on the horizontal axis for 15 minutes, the powder amount, which was 65 grams before the test, decreased to 63.66 grams at the end of the grinding, their total weight before the experiment was 240.48 grams. The weight of 115 balls with a diameter of 8 mm was measured as 240 45 grams at the end of grinding. During the experiment, which lasted for 15 minutes, the system’s energy consumption was measured as 0.572 kWh. The milling results for the Sprott-A chaotic system are presented in Table 4.

While the Pehlivan-Wei chaotic system was operated for 15 minutes at a constant speed of 25 Hz on the circular axis and a frequency varying between 33 Hz and 37 Hz on the horizontal axis, the amount of powder, which was 65 grams before the test, decreased to 64.43 grams at the end of the grinding, their total weight before the experiment was 240. The weight of 115 balls with a diameter of 8 mm, which is 45 grams, was measured as 240 42 grams at the end of grinding. During the experiment, which lasted for 15 minutes, the system’s energy consumption was measured as 0.56 kWh. The milling results for the Pehlivan-Wei chaotic system are presented in Table 5.

The best results were obtained regarding powder size and energy efficiency with the Pehlivan-Wei chaotic system in Table 5, in the experiments performed at a constant speed of 25 Hz on the circular axis and at chaotic variable speeds between 33 Hz and 37 Hz on the horizontal axis. The ground powders’ appearance is classified according to size, as shown in Figure 21.

3) INGBM’S OPERATION RESULTS WITH FIXED FREQUENCY ON THE HORIZONTAL AXIS AND CHAOTIC SYSTEM ON THE CIRCULAR AXIS

Finally, SiC powder was ground for 15 minutes at a constant speed of 35 Hz on the horizontal axis and at chaotic variable speeds between 23 Hz and 27 Hz using three different chaotic systems (Lorenz, Sprott A and Pehlivan-Wei systems) on the circular axis. Afterward, a 60-minute sieve analysis was performed. The powder size and energy efficiency were measured, and the results are shown in Table 6 for the Lorenz System, Table 7 for the Sprott-A system and Table 8 for the Pehlivan-Wei system.

While the Lorenz chaotic system was operated for 15 minutes at a constant speed of 35 Hz on the horizontal axis and a frequency varying between 23 Hz and 27 Hz on the circular axis, the powder amount, which was 65 grams before the experiment, decreased to 64.30 grams at the end of the

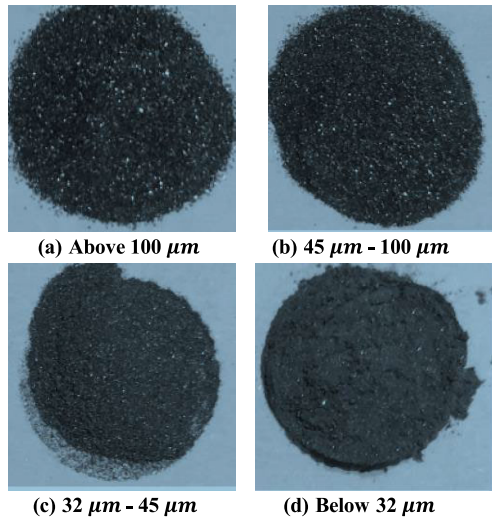


FIGURE 21. Horizontal axis (In the range of 33-37 Hz), Circular axis = 25 Hz (Constant frequency speed), Image of Ground powders with the Pehlivan-Wei chaotic system.

TABLE 6. Horizontal axis = 35 Hz (Constant frequency speed) circular axis Lorenz system (In the range of 23-27 Hz, average 25,26 Hz).

Particle Size Range (μm)	Distribution of the Powder Amount (% wt)	Distribution of the Powder Amount (g)
100 μm +	84.20 %	54.14
100 – 45 μm	12.22 %	7.86
45 – 32 μm	0.37 %	0.24
- 32 μm	3.21 %	2.06

TABLE 7. Horizontal axis = 35 Hz (Constant frequency speed), circular axis Sprott-A system (In the range of 23-27 Hz, average 25,62 Hz).

Particle Size Range (μm)	Distribution of the Powder Amount (% wt)	Distribution of the Powder Amount (g)
100 μm +	85.11 %	54.61
100 – 45 μm	12.15%	7.80
45 – 32 μm	0.78 %	0.50
- 32 μm	1.96 %	1.25

grinding, while the total weight before the experiment was 240.42 grams.

The weight of 115 balls with a diameter of 8 mm was measured as 240 40 grams at the end of grinding. During the 15-minute experiment, the system’s energy consumption was measured as 0.567 kWh. The milling results for the Lorenz system are presented in Table 6.

TABLE 8. Horizontal axis = 35 Hz (Constant frequency speed), Circular axis Pehlivan-Wei system (In the range of 23-27 Hz, average 23,51 Hz).

Particle Size Range (μm)	Distribution of the Powder Amount (% wt)	Distribution of the Powder Amount (g)
100 μm +	85.06 %	54.51
100 – 45 μm	12.14%	7.78
45 – 32 μm	0.75 %	0.48
- 32 μm	2.04 %	1.31

Sprott A chaotic system with a constant speed of 35 Hz on the horizontal axis and a frequency varying between 23 Hz and 27 Hz on the circular axis for 15 minutes, the powder amount, which was 65 grams before the test, decreased to 64.16 grams at the end of the grinding, their total weight before the experiment was 240.40 grams.

The weight of 115 balls with a diameter of 8 mm was measured as 240.38 grams at the end of grinding. During the experiment, which lasted for 15 minutes, the system’s energy consumption was measured as 0.56 kWh. The milling results for the Sprott A system are presented in Table 7.

While the Pehlivan-Wei chaotic system was operated for 15 minutes at a constant speed of 35 Hz on the horizontal axis and at a frequency ranging from 23 Hz to 27 Hz on the circular axis, the amount of powder, which was 65 grams before the test, decreased to 64.08 grams at the end of the grinding, their total weight before the experiment was 240.

The weight of 115 balls with a diameter of 8 mm, which is 38 grams, was measured as 240.36 grams at the end of grinding. During the experiment, which lasted for 15 minutes, the system’s energy consumption was measured as 0.56kWh. The milling results for the Pehlivan-Wei system are presented in Table 8.

The best results were obtained regarding powder size and energy efficiency criteria with the Lorenz chaotic system in Table 6 in the experiments performed at a constant speed of 35 Hz on the horizontal axis and at chaotic variable speeds between 23 Hz and 27 Hz on the circular axis. The ground powders’ appearance is classified according to size, as shown in Figure 22.

In addition, at the end of the milling processes, it was observed that the powders flew when the powder container was opened. As a result of this observation, it is noted that the ground powder is reduced to nano dimensions.

B. SCANNING ELECTRON MICROSCOPY (SEM) OF THE GROUND POWDERS

SEM images for the morphological examination of SiC powders milled by the sieve analysis method in different chaotic systems and at constant frequency speeds are given in Figure 23 and Figure 24. The initial size of the ground powders was around 100-150 microns. After grinding with

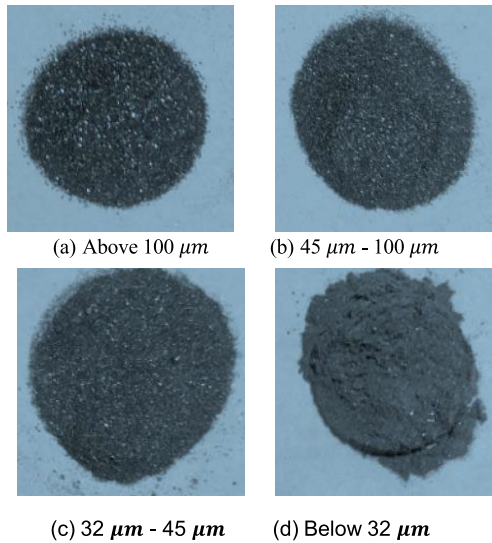


FIGURE 22. Horizontal axis (In the range of 33-37 Hz), Circular axis = 25 Hz (Constant frequency speed), Image of Ground powders with the Pehlivan-Wei chaotic system.

different parameters and chaotic models, the size differences between SiC powders are clearly visible in the SEM images.

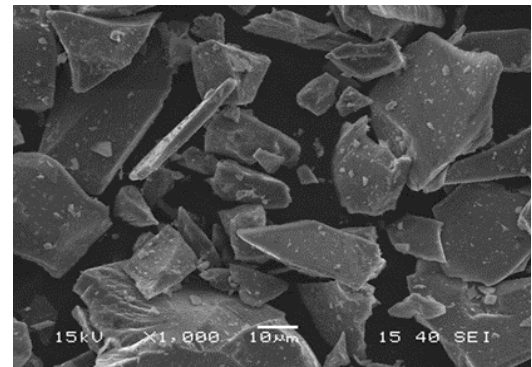
1) SEM RESULTS OF OPERATING WITH A CHAOTIC SYSTEM ON THE HORIZONTAL AXIS AND FIXED FREQUENCY ON THE CIRCULAR AXIS

Powders ground with the circular axis chaotic and the horizontal axis constant frequency speed in Figure 23 were milled from a size of 100-150 microns to approximately 30-60 microns.

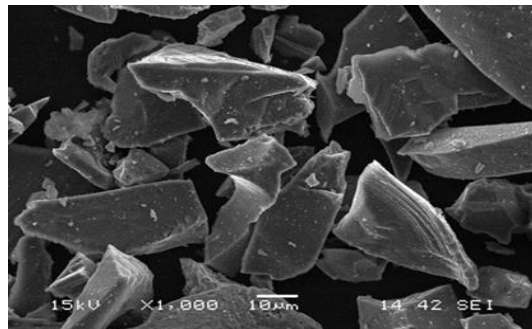
In grinding with the integration of the Sprott-A chaotic model, a noticeable reduction in particle sizes of approximately 10-15 microns was observed in Figure 23 (c). It can be seen that the sizes and morphologies of the ground powders obtained by using the Pehlivan model are similar to Figure 23 (b) for the Sprott-A model. A bimodal particle size distribution is observed in the grinding performed by integrating the Lorenz chaotic model given in Figure 23 (a). However, the powder size distribution range is wide, from 50 microns to submicron levels. According to the sieve analysis results performed after the powder grinding process, the highest percentage of powder below 32 μm was seen in the Lorenz chaotic system. A similar result was revealed in the SEM images made in this section. It can be seen that the Lorenz chaotic system is more efficient when the circular axis is the chaotic system, and the horizontal axis is kept at a constant frequency rate.

2) SEM RESULTS OF OPERATING WITH A FIXED FREQUENCY ON THE HORIZONTAL AXIS AND CHAOTIC SYSTEM ON THE CIRCULAR AXIS

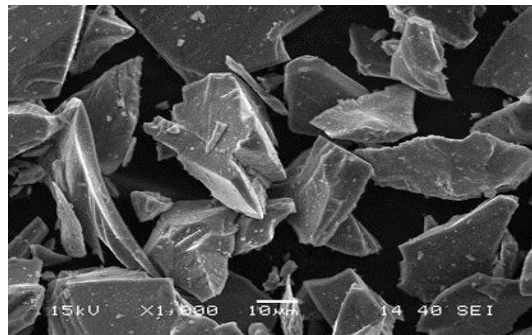
Figure 24 (a), (b) and (c) shows the SEM images of the powders ground with a chaotic system on the horizontal axis, keeping the orbital axis constant frequency speed.



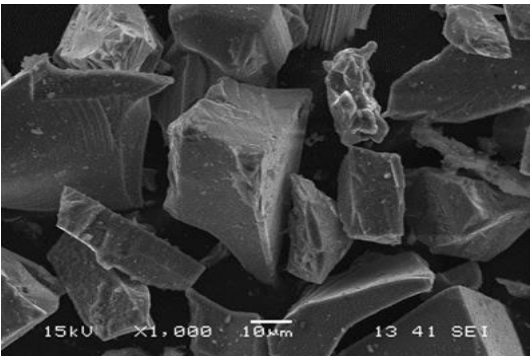
(a) Horizontal Axis = 35 Hz (Constant frequency speed), Circular Axis Lorenz System (In the range of 23-27 Hz),



(b) Horizontal Axis = 35 Hz (Constant frequency speed), Circular Axis Pehlivan-Wei System (In the range of 23-27 Hz),

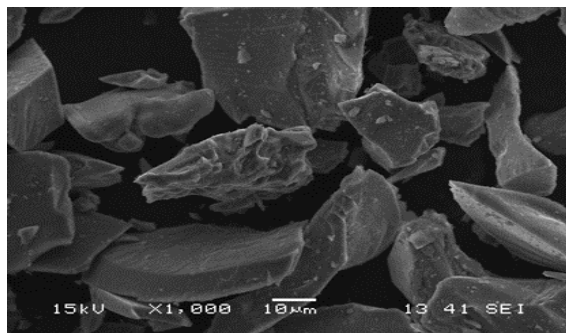


(c) Horizontal Axis = 35 Hz (Constant frequency speed), Circular Axis Sprott-A System (In the range of 23-27 Hz),

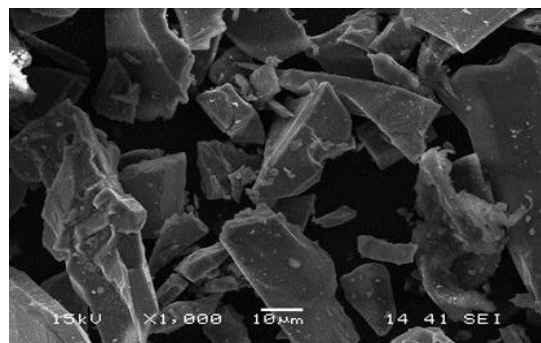


(d) Horizontal Axis = 35 Hz (Constant frequency speed), Circular Axis = 25 Hz (Constant frequency speed),

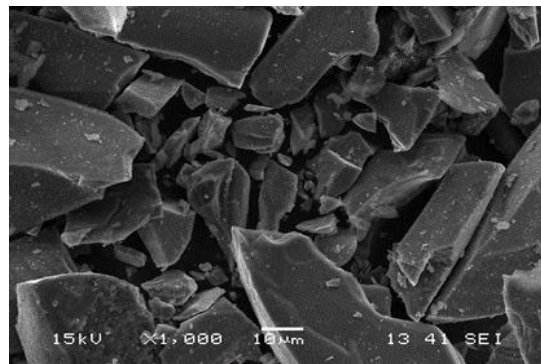
FIGURE 23. SEM images of powders ground with the circular axis chaotic and the horizontal axis constant frequency speed (a, b and c) and the powder ground without integrating the chaotic system (d).



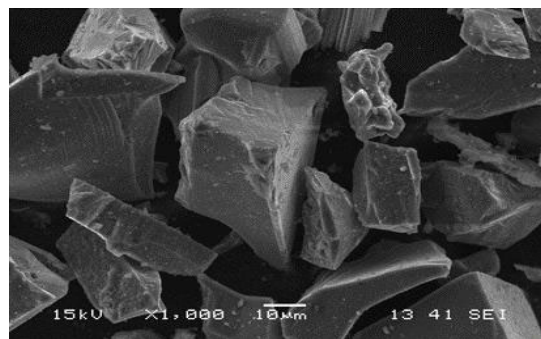
(a) Horizontal Axis Lorenz System (In the range of 33-37 Hz), Circular Axis = 25 Hz (Constant frequency speed),



(b) Horizontal Axis Pehlivan-Wei System (In the range of 33-37 Hz), Circular Axis = 25 Hz (Constant frequency speed).



(c) Horizontal Axis Sprott-A System (In the range of 33-37 Hz), Circular Axis = 25 Hz (Constant frequency speed),



(d) Horizontal Axis= 35 Hz (Constant frequency speed), Circular Axis= 25 Hz (Constant frequency speed).

FIGURE 24. SEM images of chaotically ground powders (a, b and c) with circular axis constant frequency speed and horizontal axis and powder ground without integrating the chaotic system (d).

As mentioned in Section III-A1, the ground powders in the reference system -operated at constant speeds in the orbital and linear axis- ranging from 100-150 microns in size to approximately 30-60 microns. When the chaotic integration was made to the horizontal axis instead of the circular, unlike the previous one, the most efficient grinding was obtained with the Sprott-A and Pehlivan-Wei chaotic models. As can be seen in the SEM image in Figure 24 (b), (c), it can be seen that the powders milled in the Sprott-A and Pehlivan-Wei chaotic systems transform into finer grain sizes and a dual-mode powder size clustering is clearly seen. Similarly, in the sieve analysis method, the highest amount passing through the 32-micron sieve was again obtained when Sprott-A and Pehlivan-Wei chaotic models were used.

As seen in Sections III-A and III-B, a more positive grinding efficiency was observed in both SEM images and Sieve analysis methods in the chaotic system integrated INGBM than in the non-chaotic NGBM.

IV. SUMMARY OF THE EXPERIMENTAL RESULTS

In our study, first of all, traditional ball mills (TBM) and new generation ball mills (NGBM) are compared and the information that NGBM is more efficient than TBM is presented. Later, a new control unit was created at NGBM using new versions of PLC and inverters. An independent control panel was created outside the grinder for the control unit, which was previously inside the grinding machine and was negatively affected by vibration. In addition, the system was modernized to work with chaotic signals and the Improved New Generation Ball Mill (INGBM) was produced. In experimental studies, INGBM was operated initially with a fixed frequency and subsequently with chaotic signals on the horizontal and circular axes. Experimental results revealed the efficiency of the INGBM integrated with the chaotic system in terms of powder size and energy consumption criteria.

Silicon Carbide (SiC) powder was ground with INGBM, which was modernized by integrating the chaotic system. In the experiments, the ball mill was initially operated at constant frequency speeds in horizontal and circular axes and the results were obtained. In the second stage, experiments were carried out with three different chaotic systems by operating the horizontal axis at a constant speed and integrating the circular axis chaotic system. In the last stage, Experiments were carried out by operating the horizontal axis by integrating the chaotic system and operating the circular axis at a constant speed. SiC powders separated by sieve analysis were also analyzed using the SEM method.

Experiments were conducted with INGBM using Silicon Carbide (SiC) powders with different frequency parameters and operating times. The optimum value for frequency parameters is 35 Hz on the horizontal axis and 25 Hz on the circular axis. In repeated experiments, it is observed that the chaotic system integrated ball mill is efficient.

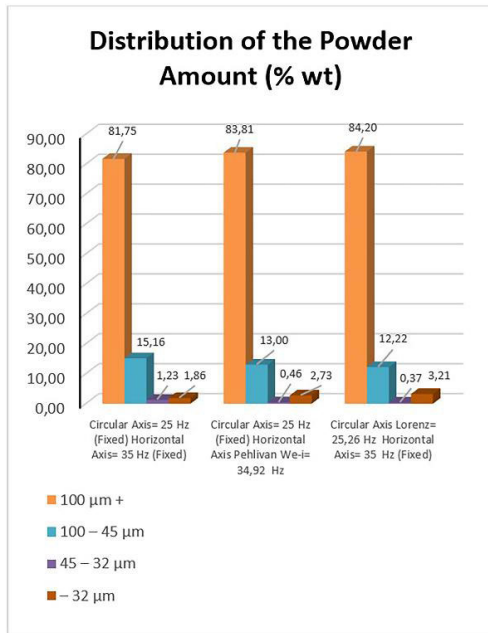


FIGURE 25. Comparison of the powder milling process results of running INGBM with constant frequency speed and chaotic motion.

Powder size data obtained by the Sieve analysis method in Section III-A is shown in the graph in Figure 25.

When the horizontal and circular axes are moved at a constant frequency speed in INGBM, the amount of dust below $32 \mu\text{m}$ is 1.86%.; When the horizontal axis is operated with the Pehlivan-Wei chaotic system and the circular axis is operated with a constant frequency speed, the amount of dust below $32 \mu\text{m}$ is 2.73%. When the horizontal axis is operated at a fixed frequency of 35 Hz and the circular axis is operated with the Lorenz chaotic system, this rate is 3.21%. The scenario of operating the INGBM at constant frequency speed in both axes compared the scenario in which the chaotic system integrated in the circular axis. The results showed that the chaotic system integrated ball mill (INGBM) is 42% more efficient than non-chaotic scenario in the powder size criterion.

A similar situation is observed in the SEM analyses in Section III-B. When the SEM images were examined, it was observed that the SIC powders were divided into smaller pieces in the ball mill operated by integrating the chaotic system, compared to the ball mill operating at constant speeds. This shows that the chaotic system integrated ball mill is more efficient, as in the Sieve analysis method.

Calculating the average current draw and, therefore, the energy consumption of INGBM for each different operating scenario is mentioned in Section II-C1.

The data obtained for all three options is specified in Section III-A, where the experimental results shown in the energy efficiency criterion are shown in the graph in Figure 26.

The energy consumed while the horizontal and circular axes operated at constant frequency speed in INGBM was measured as 0.58 kWh.

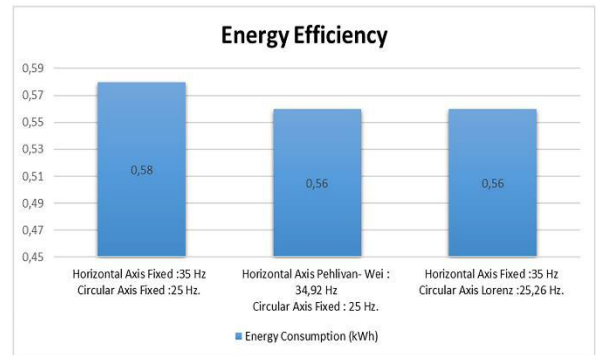


FIGURE 26. Comparison of the energy efficiency results with running INGBM at constant frequency speed and chaotic motions.

When the horizontal axis operated with the Pehlivan-Wei chaotic system and the circular axis operated at a constant speed of 25 Hz, the amount of energy consumed was measured as 0.56 kWh.

When the horizontal axis was operated at a constant speed of 35 Hz and the circular axis was operated with the Lorenz chaotic system, the amount of energy consumed was measured as 0.56 kWh.

The results reveal that the chaotic system integrated improved ball mill, INGBM, is 3.44% more efficient than conventional ball mill, in terms of energy efficiency.

Sections III-A and III-B show that SIC powders milled in chaotic integrated INGBM were analyzed using SEM and sieve analysis methods. As a result of the analysis, grinding results with chaotic system integrated INGBM are observed to be more efficient in powder size and energy efficiency criteria than non-chaotic NGBM.

V. CONCLUSION

The NGBM is quite efficient compared to the ball mills in its class, which are conventional-type ball mills and planetary-type mills. In this research article, modernization has been carried out by ensuring that the current new-generation ball mill (NGBM) is operated on a chaotic basis.

Then, experimental studies were carried out using modernized INGBM. Experiments were conducted with INGBM using Silicon Carbide (SIC) powders with different frequency parameters and operating times.

This study focusing on reducing powder sizes by consuming less energy. The ground powders by the INGBM were examined using sieve analysis and SEM analysis methods. The results of both methods revealed that the chaotic system integrated ball mill (INGBM) is quite efficient compared to traditional ball mills (NGBM) in terms of powder size and energy efficiency.

When the horizontal axis is operated at a fixed frequency of 35 Hz and the circular axis is operated with the Lorenz chaotic system, amount of dust below $32 \mu\text{m}$ is 3.21%. The scenario of operating the INGBM at constant frequency speed in both axes compared the scenario in which the chaotic system integrated in the circular axis. The results showed

that the chaotic system integrated ball mill (INGBM) is 42% more efficient than non-chaotic scenario in the powder size criterion.

In future studies, experimental studies will be conducted with different materials (For example, Alumina) and by integrating different chaotic systems into INGBM.

Many approaches to noise generation, with variable noise color, spectrum distribution and intensity, white noise and pseudo-random generators, are valuable scientific data for randomness. In addition to these scientific data, we plan to use various entropy sources (e.g., ambient temperature noise, noise on digital integrated circuits, noise in communication systems, etc.) in addition to the current chaos sources to control motor movements. Besides, within the scope of this study, we aim to observe the effects of chaotic oscillators and added entropy sources on the system more clearly by constantly monitoring them through feedback sensors.

ACKNOWLEDGMENT

The authors would like to thank Sakarya University of Applied Sciences, Scientific Research Projects Coordinators for their contribution to the following Scientific Research Projects by providing material and device support;

“2021-01-04-057-Design and Performance Analysis of a New Chaos Based Mechanical Grinder” and “123-2023-Design and Analysis of a Chaos-Based New Generation Ball Mill.”

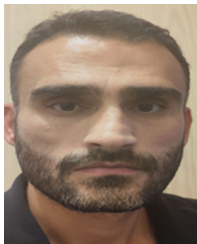
REFERENCES

- [1] F. Monteverde, “Beneficial effects of an ultra-fine α -SiC incorporation on the sinterability and mechanical properties of ZrB₂,” *Appl. Phys. A, Solids Surf.*, vol. 82, no. 2, pp. 329–337, Feb. 2006.
- [2] M. Bengisu, *Ceramic Science and Engineering*. Ankara, Turkey: Nobel Publication Distribution, 2006.
- [3] M. Somiya, *Silicon Carbide Ceramics*. London, U.K.: Springer, 1991.
- [4] P. T. Shaffer, *Handbook of Advanced Ceramic Materials*. New York, NY, USA: Advanced Refractory Technologies, Inc., 1991.
- [5] H. O. Pierson, *Handbook of Refractory Carbides and Nitrides*. Saddle River, NJ, USA: Noyes Publications, 1996.
- [6] Z. C. Feng and J. H. Zhao, *Silicon Carbide Materials*. New York, NY, USA: Taylor and Francis, 2000.
- [7] F. Cinar, D. Gençkan, and O. Yucel, “Spark plasma sintering of B₄C-SiC composites,” *Solid State Sci.*, vol. 14, pp. 1660–1663, Nov. 2012.
- [8] W. B. Eisen, B. L. Ferguson, R. M. German, R. Iacocca, P. W. Lee, D. Madan, K. Moyer, H. Sanderow, and Y. Trudel, *Powder Metal Technologies and Applications*. Materials Park, OH, USA: ASM International, 1998.
- [9] H. H. Hausner, *Modern Developments in Powder Metallurgy*. New York, NY, USA: Springer, 1966.
- [10] G. S. Upadhyaya, *Powder Metallurgy Technology*. Cambridge, U.K.: Cambridge International Science Publishing, 1997.
- [11] M. Paul, Y. Alshammari, F. Yang, and L. Bolzoni, “New ternary powder metallurgy Ti alloys via eutectoid and isomorphous beta stabilisers additions,” *Sci. Rep.*, vol. 13, no. 1, Jan. 2023, Art. no. 1150.
- [12] A. Onur, “Investigation of metal powder production by oil atomization method,” Ph.D. thesis, Dept. Mech. Eng., Karadeniz Technical Univ., Inst. Sci., Trabzon, Turkey, 1996.
- [13] A. Lawley, *Atomization: The Production of Metal Powders*. Princeton, NJ, USA: Metal Powder Industries Federation, 1992.
- [14] R. K. Dhir, J. Brito, R. V. Silva, and C. Q. Lye, *Sustainable Construction Materials: Recycled Aggregate*. New York, NY, USA: Springer, 2019.
- [15] G. Atesok, N. A. Mütevelioğlu, H. Dinçer, and F. Ve Boylu, “The effect of some dispersive chemicals on the grindability of coals, mining,” *Madençilik*, vol. 44, pp. 25–35, Jan. 2005.
- [16] S. Ellis and M. Gao, “Development of ultrafine grinding at Kalsoorlie consolidated gold mines,” *Mining, Metall. Explor.*, vol. 20, no. 4, pp. 171–177, Nov. 2003.
- [17] A. Jankovic, “Variables affecting the fine grinding of minerals using stirred mills,” *Minerals Eng.*, vol. 16, no. 4, pp. 337–345, Apr. 2003.
- [18] S. Dikmen and S. L. Ergün, “Stirred ball mills,” *Sci. Mining J.*, vol. 43, pp. 3–15, Jan. 2004.
- [19] H. Demirel, *Milling Mineral Processing Handbook*. Istanbul, Turkey: Yurt Mining Development Foundation Publications, 1994.
- [20] H. Gungordu, “Design and investigation of new type mechanical mixer in powder metallurgy,” M.S. thesis, Inst. Sci. Technol., Sakarya Univ., Sakarya, Turkey, 2008.
- [21] I. Pehlivan, “New chaotic systems: Electronic circuit implementations, synchronization and secure communication applications,” Ph.D. thesis, Sakarya Univ., Inst. Sci. Technol., Sakarya, Türkiye, 2007.
- [22] A. Akgül, “Random number generator design with new chaotic systems and high security encryption of multimedia data,” Ph.D. thesis, Inst. Sci. Technol., Sakarya Univ., Sakarya, Türkiye, 2015.
- [23] O. Kalayci, I. Pehlivan, and S. Coşkun, “Improving the performance of industrial mixers that are used in agricultural technologies via chaotic systems and artificial intelligence techniques,” *Turkish J. Electr. Eng. Comput. Sci.*, vol. 30, no. 6, pp. 2418–2432, Sep. 2022.
- [24] I. Pehlivan and Z. Wei, “Analysis, nonlinear control, and chaos generator circuit of another strange chaotic system,” *Turkish J. Electr. Eng. Comput. Sci.*, vol. 20, pp. 1229–1239, Jan. 2012.
- [25] E. N. Lorenz, “Deterministic nonperiodic flow,” *J. Atmos. Sci.*, vol. 20, no. 2, pp. 130–141, Mar. 1963.
- [26] P. Güven, “Random number generation at the non-autonomous chaotic systems,” M.S. thesis, Istanbul Technical Univ., Inst. Sci. Technol., Istanbul, Turkey, 2006.
- [27] L. O. Chua, C. W. Wu, A. Huang, and G.-Q. Zhong, “A universal circuit for studying and generating chaos. I. Routes to chaos,” *IEEE Trans. Circuits Syst. I, Fundam. Theory Appl.*, vol. 40, no. 10, pp. 732–744, Oct. 1993.
- [28] S. Mobayen, A. Fekih, S. Vaidyanathan, and A. Sambas, “Chameleon chaotic systems with quadratic nonlinearities: An adaptive finite-time sliding mode control approach and circuit simulation,” *IEEE Access*, vol. 9, pp. 64558–64573, 2021.
- [29] G. Chen and T. Ueta, “Yet another chaotic attractor,” *Int. J. Bifurcation Chaos*, vol. 9, no. 7, pp. 1465–1466, Jul. 1999.
- [30] J. C. Sprott, “Simple chaotic flows,” *Phys. Rev. E, Stat. Phys. Plasmas Fluids Relat. Interdiscip. Top.*, vol. 50, pp. 647–650, Jun. 1994.
- [31] M. Alçın, M. Tuna, I. Pehlivan, and I. Koyuncu, “CCII current conveyor and dormant-prince-based chaotic oscillator designs for secure communication applications,” *Int. Adv. Researches Eng. J.*, vol. 4, no. 3, pp. 217–225, Dec. 2020.
- [32] Ü. Çavuşoğlu, S. Kaçar, A. Zengin, and I. Pehlivan, “A novel hybrid encryption algorithm based on chaos and S-AES algorithm,” *Nonlinear Dyn.*, vol. 92, no. 4, pp. 1745–1759, Jun. 2018, doi: 10.1007/s11071-018-4159-4.
- [33] B.-W. Shen, R. A. Pielke, X. Zeng, J.-J. Baik, S. Faghig-Naini, J. Cui, and R. Atlas, “Is weather chaotic: Coexistence of chaos and order within a generalized Lorenz model,” *Bull. Amer. Meteorolog. Soc.*, vol. 102, no. 1, pp. E148–E158, Jan. 2021.
- [34] S. Coşkun, I. Pehlivan, A. Akgül, and B. Gürevin, “A new computer-controlled platform for ADC-based true random number generator and its applications,” *TURKISH J. Electr. Eng. Comput. Sci.*, vol. 27, pp. 847–860, Mar. 2019.
- [35] O. Kalayci, I. Pehlivan, and S. Coskun, “Improving the performance of mixers used in humic acid production with chaotic systems,” *Turkish J. Agricul. Food Sci. Technol.*, vol. 9, pp. 508–514, Jan. 2021.
- [36] O. Kalayci, I. Pehlivan, A. Akgul, S. Coskun, and E. Kurt, “A new chaotic mixer design based on the delta robot and its experimental studies,” *Math. Problems Eng.*, vol. 2021, pp. 1–15, Mar. 2021.
- [37] E. Kurt, “A new chaotic mixer design and application,” M.S. thesis, Inst. Sci. Technol., Mechatronics Eng., Sakarya Univ., Sakarya, Turkey, 2017.
- [38] K. T. Chau, S. Ye, Y. Gao, and J. H. Chen, “Application of chaotic-motion motors to industrial mixing processes,” in *Proc. Conf. Rec. IEEE Ind. Appl. Conf., 39th IAS Annu. Meeting.*, Seattle, WA, USA, Oct. 2004, pp. 1874–1880.
- [39] S. Ye and K. T. Chau, “Destabilization control of a chaotic motor for industrial mixers,” in *Proc. 40th IAS Annu. Meeting. Conf. Rec. Ind. Appl. Conf.*, Hong Kong, Oct. 2005, pp. 1724–1730.

- [40] M. A. Murtadha, M. Abdurrahman, and A. I. Korman, "Chaotic control of liquid mixer," Senior Des. Project II, Dept. Elect. Comput. Eng., Univ. Sharjah, Sharjah, UAE, 2008.
- [41] Z. Zhang and G. Chen, "Liquid mixing enhancement by chaotic perturbations in stirred tanks," *Chaos, Solitons Fractals*, vol. 36, no. 1, pp. 144–149, Apr. 2008.
- [42] A. E. Kavur, S. Demiroglu, M. Ö. Seydibeyoglu, Ö. Baser, C. Güzelis, and S. Sahin, "Design and implementation of chaotic system based robust delta robot for blending graphene nanoplatelets," in *Proc. 21st Int. Conf. Methods Models Autom. Robot. (MMAR)*, Aug. 2016, pp. 235–240.
- [43] I. Koyuncu, A. T. Ozcerit, and I. Pehlivan, "Implementation of FPGA-based real time novel chaotic oscillator," *Nonlinear Dyn.*, vol. 77, nos. 1–2, pp. 49–59, Jul. 2014.



conference papers. His research interests include dynamic systems, chaos, chaotic systems, chaotic industrial mixers, and chaotic industrial ball mills.



conference papers. His research interests include dynamic systems, chaos, chaotic systems, chaotic industrial mixers, chaotic industrial grinders, and fuzzy logic.



programming of control systems. He has more than 80 articles to his credit.



ate, Sakarya University of Applied Sciences. He currently works as a Mechanical Design Engineer with the Research and Development Department of a private company.



the author of four SCI articles and three conference papers. His research interests include digital electronics, analog electronics, embedded systems, microcontrollers, programming, IoT systems, digital agriculture, chaotic systems, and random number generators.



Currently, he is a Professor of materials science engineering with Sakarya University of Applied Sciences, Turkey. In recent years, he has focused on powder metallurgy, bioceramics, nanocomposites, radiation shielding, and Industry 4.0 applications. He is currently conducting many projects on these areas.



patents. His research interests include analog electronic circuits, dynamical systems, chaos, chaotic systems, circuit theory, electronic circuit realizations of chaotic systems, chaotic oscillators, synchronization of chaotic systems, chaotic secure communication systems and circuits, random number generators, FPGA based chaotic circuits, FPGA based random number generators, chaotic industrial mixers, chaotic industrial grinders, and fuzzy logic.



control, optimal control, mathematical modeling, and scientific computing.

...